Biosensors and Bioelectronics 100 (2018) 583–590

Contents lists available at ScienceDirect

Biosensors and Bioelectronics

journal homepage: www.elsevier.com/locate/bios

A sensitive biosensor using double-layer capillary based immunomagnetic separation and invertase-nanocluster based signal amplification for rapid detection of foodborne pathogen

Fengchun Huang[a], Huilin Zhang[a], Lei Wang[a], Weihua Lai[b], Jianhan Lin[c,*]

[a] Key Laboratory of Agricultural Information Acquisition Technology, Ministry of Agriculture, China Agricultural University, 17 East Qinghua Road, Beijing 100083, China
[b] State Key Laboratory of Food Science and Technology, Nanchang University, 235 Nanjing East Road, Nanchang 330047, China
[c] Key Laboratory on Modern Precision Agriculture System Integration Research, Ministry of Education, China Agricultural University, 17 East Qinghua Road, Beijing 100083, China

ARTICLE INFO

Keywords:
Biosensor
Double-layer capillary
Invertase nanoclusters
High gradient magnetic separation
Glucose meter
E. coli O157:H7

ABSTRACT

Combining double-layer capillary based high gradient immunomagnetic separation, invertase-nanocluster based signal amplification and glucose meter based signal detection, a novel biosensor was developed for sensitive and rapid detection of *E. coli* O157:H7 in this study. The streptavidin modified magnetic nanobeads (MNBs) were conjugated with the biotinylated polyclonal antibodies against *E. coli* O157:H7 to form the immune MNBs, which were captured by the high gradient magnetic field in the double-layer capillary to specifically separate and efficiently concentrate the target bacteria. Calcium chloride was used with the monoclonal antibodies against *E. coli* O157:H7 and the invertase to form the immune invertase-nanoclusters (INCs), which were used to react with the target bacteria to form the MNB-bacteria-INC complexes in the capillary. The sucrose was then injected into the capillary and catalyzed by the invertase on the complexes into the glucose, which was detected using the glucose meter to obtain the concentration of the glucose for final determination of the *E. coli* O157:H7 cells in the sample. A linear relationship between the readout of the glucose meter and the concentration of the *E. coli* O157:H7 cells (from 10^2 to 10^7 CFU/mL) was found and the lower detection limit of this biosensor was 79 CFU/mL. This biosensor might be extended for the detection of other foodborne pathogens by changing the antibodies and has shown the potential for the detection of foodborne pathogens in a large volume of sample to further increase the sensitivity.

1. Introduction

Escherichia coli O157:H7 (*E. coli* O157:H7) is one kind of considerable dangerous pathogenic bacterium, which has received great attention due to its significant impact in the fields of food safety, disease control, and environmental protection, etc. The outbreaks of *E. coli* O157:H7 have often occurred worldwide (WHO, 2015; Sharapov et al., 2016; Zhang et al., 2015) and resulted in serious public health issues and numerous economic losses, since it has been found in various contaminated foods, such as milk products (Ahmed and Shimamoto, 2015), ground beef (Torso et al., 2015) and leafy vegetables (Delaquis et al., 2007), etc. The key to prevent and control the outbreaks of foodborne diseases is rapid screening of the contaminated foods. Many traditional methods have been used to detect the foodborne pathogenic bacteria, such as bacterial culture (Voetsch et al., 2004), enzyme linked immunosorbent assay (ELISA) (Zhang et al., 2016) and polymerase chain reaction (PCR) (Gilbert et al., 2015). However, these methods either are time-consuming, or lack sensitivity, or require expensive facilities and well-trained personnel. Thus, it is of great importance to develop new rapid and sensitive methods for the detection of pathogenic bacteria.

In the past decades, various types of biosensors, such as quartz crystal microbalance (QCM) (Dong and Zhao, 2015; Nicola Luigi et al., 2015; Ozalp et al., 2015), surface plasmon resonance (SPR) (Song et al., 2017; Vaisocherová-Lísalová et al., 2016; Wang et al., 2016b), optical (Khang et al., 2016; Ren et al., 2017; Ghadeer et al., 2016), and electrochemical (Huang et al., 2016; Li et al., 2015; Xu et al., 2016), etc., have been reported for foodborne pathogen detection with the advantages of high sensitivity, good specificity, short detection time, simple operation or low cost. Magnetic nanobeads (MNBs), which are conjugated with biological recognition elements, have been widely used with different biosensors for specific separation and efficient

* Corresponding author.
E-mail address: jianhan@cau.edu.cn (J. Lin).

http://dx.doi.org/10.1016/j.bios.2017.10.005
Received 16 August 2017; Received in revised form 23 September 2017; Accepted 2 October 2017
Available online 03 October 2017

concentration of the foodborne pathogenic bacteria from the complex sample based on the antigen-antibody reaction to increase the sensitivity and specificity of the biosensors. So far, immunomagnetic separation was often performed using a magnetic field and low protein adsorption centrifuge tubes to handle biological samples with a volume of 1 mL or less (Wang et al., 2016a). However, many foodborne pathogens, including *E. coli* O157:H7, are required by China's food safety national standards to be not detectable in foods, indicating that the sensitivity of bacteria detection methods has to be very high. For the purpose of increasing the sensitivity, high gradient magnetic separation (HGMS), which often uses the magnetizable wires or balls in the separation channel to capture the immune MNBs at the presence of the magnetic field for reacting with the biological targets, has been reported to separate the biological targets from a large volume of sample and concentrate them in a small volume of buffer solution, and demonstrated to be effective way to increase the sensitivity (Lin et al., 2015; Zheng et al., 2015; García et al., 2015). However, the non-specific binding of the proteins to the wires or balls and the blocking of the channel by the large particles in the sample have greatly limited its practical applications. Thus, new methods for efficient separation of the target bacteria from large volume (10 mL or more) of sample are needed.

Besides, various enzymes, such as glucose oxidase (Zhang et al., 2014), urease (Chen et al., 2016) and peroxidase (Chen et al., 2014), etc., have been widely used to amplify the biological signals for improving the sensitivity of the biosensors on the detection of foodborne pathogens or other small biomolecules. The commonly-used strategy is ELISA (Zhu et al., 2016) or related methods, which often immobilize the antibodies on the solid phase to capture the targets followed by the antibodies' reacting with the enzyme modified pair antibodies to form the sandwich complexes and the enzyme's catalyzing the subtract into another color for the determination of the targets. Another popular strategy often uses the gold nanoparticles to conjugate with both the antibodies and the enzymes for reacting with the targets, followed by detecting the catalysate to determine the amount of the targets (Chen et al., 2015). However, the activities of the enzymes and the antibodies might be partially lost due to the steric hindrance, resulting in the decrease of the immunoreaction efficiency and the catalysis efficiency. A facile one-step coprecipitation method was reported for the synthesis of the organic-inorganic hybrid nanoclusters, using copper (II) ions as the inorganic component and different proteins as the organic component, and has received great attention (Ge et al., 2012). The nanoclusters have been demonstrated to be able to remarkably amplify the signals due to their large surface-to-volume ratio, resulting in higher binding capacity for the enzymes. Based on this concept, several studies were reported for the detection of foodborne pathogens using concanavalin A-glucose oxidase-$Cu_3(PO_4)_2$ nanoclusters (Ye et al., 2016) or antibody-horseradish peroxidase-$Cu_3(PO_4)_2$ nanoclusters (Wei et al., 2016).

In this study, we described a novel biosensor using double-layer capillary based immunomagnetic separation, invertase-nanocluster based signal amplification, and glucose meter based signal detection for sensitive and rapid detection of foodborne pathogen and used *E. coli* O157:H7 as research model to evaluate this proposed biosensor. Prior to test, the streptavidin modified magnetic nanobeads were conjugated with the biotinylated polyclonal antibodies (pAbs) against *E. coli* O157:H7 to prepare the immune MNBs, and calcium chloride ($CaCl_2$) was mixed with the monoclonal antibodies (mAbs) against *E. coli* O157:H7 and the invertase to prepare the immune invertase-nanoclusters (INCs) (see Fig. 1(A)). As shown in Fig. 1(B) and (C), the immune MNBs were first injected into the double-layer capillary and were distributed uniformly in the capillary at the presence of the high gradient magnetic fields (HGMFs). The *E. coli* O157:H7 cells were captured by the immune MNBs through antigen-antibody reaction, when they flowed through the capillary. Then, the immune INCs were injected to react with the target bacteria, resulting in the forming of the MNB-bacteria-INC complexes in the capillary. After the sucrose was injected into the capillary and catalyzed into the glucose by the invertase on the complexes, the glucose was detected using the glucose meter to determine the concentration of the glucose and the amount of the *E. coli* O157:H7 cells in the sample could be obtained based on the calibration curve of the proposed biosensor.

2. Materials and methods

2.1. Materials

Phosphate buffered saline (PBS, 10 mM, pH 7.4) from Sigma-Aldrich (St. Louis, MO, USA) was used as buffer solution. Calcium chloride from XiLong Scientific (Shantou, Guangdong, China) was used for the synthesis of the nanoclusters. Bovine serum albumin (BSA) from Sigma-Aldrich was prepared with PBS (10% and 1.0%, w/v) as blocking solution. The biotinylated polyclonal antibodies (4–5 mg/mL) from Meridian (Cincinnati, OH, USA) and the monoclonal antibodies (2.19 mg/mL) developed by Nanchang University were used for immunological reaction with the *E. coli* O157:H7 cells since they had different antigen binding sites and could react with the same bacterial cell with less steric hindrance and competition. The western blotting kit from KPL (Gaithersburg, MD, USA) was used for Dot-ELISA analysis. Invertase from Sigma-Aldrich was used for catalyzing the sucrose into the glucose. The commercial glucose meter (Type: OneTouch, glucose detection range: 1.1–33.3 mM) and test trips from LifeScan (Milpitas, CA, USA) were used for the determination of glucose concentration. The streptavidin modified magnetic nanobeads with the diameter of 150 nm from Ocean NanoTech (Springdale, AR, USA) were used for capturing and separating the *E. coli* O157:H7 cells from the sample. Other reagents from Sinopharm Chemical (Shanghai, China) were of analytical grade. The deionized water produced by Advantage A10 from Millipore (Billerica, MA, USA) was used to prepare all the solutions.

2.2. Preparation of the bacterial cultures

In this study, *E. coli* O157:H7 (ATCC43888) was used as the model target bacteria for the proof of the concept and *Salmonella typhimurium* (*S. typhimurium,* ATCC14028) was used as the model non-target bacteria for the evaluation of the specificity. They were both stored with 15% glycerol at −20 °C and revived on Luria-Bertani (LB) agar plates. Their cultures were grown in LB medium (Aoboxing Biotech, Beijing, China) at 37 °C for 12–18 h with shaking at 180 rpm, respectively. For obtaining the bacteria with the concentrations ranging from 10^1 to 10^7 CFU/mL, the cultures were serially 10-fold diluted with the sterile PBS. For enumerating the bacteria, the bacterial sample was serially diluted with the sterile PBS, and surface plated on the LB agar plates, followed by incubation at 37 °C for 22–24 h and counting of the visible colonies.

2.3. Synthesis of the immune invertase-nanoclusters

The nanoclusters were synthesized based on the one-step co-precipitation method reported by Ge with some modifications (Ge et al., 2012). Briefly, 100 μL of the mAbs against *E. coli* O157:H7 (0.219 mg/mL) and 18 μL of the invertase (10 mg/mL) were successively added into 1 mL of PBS (3 mM, pH 6.8). Then, 20 μL of $CaCl_2$ (200 mM) was added and incubated for 12 h at room temperature. The prepared immune INCs were obtained through centrifugation at 15,000 rpm for 5 min, washed with the deionized water three times, and finally stored at −20 °C for further use.

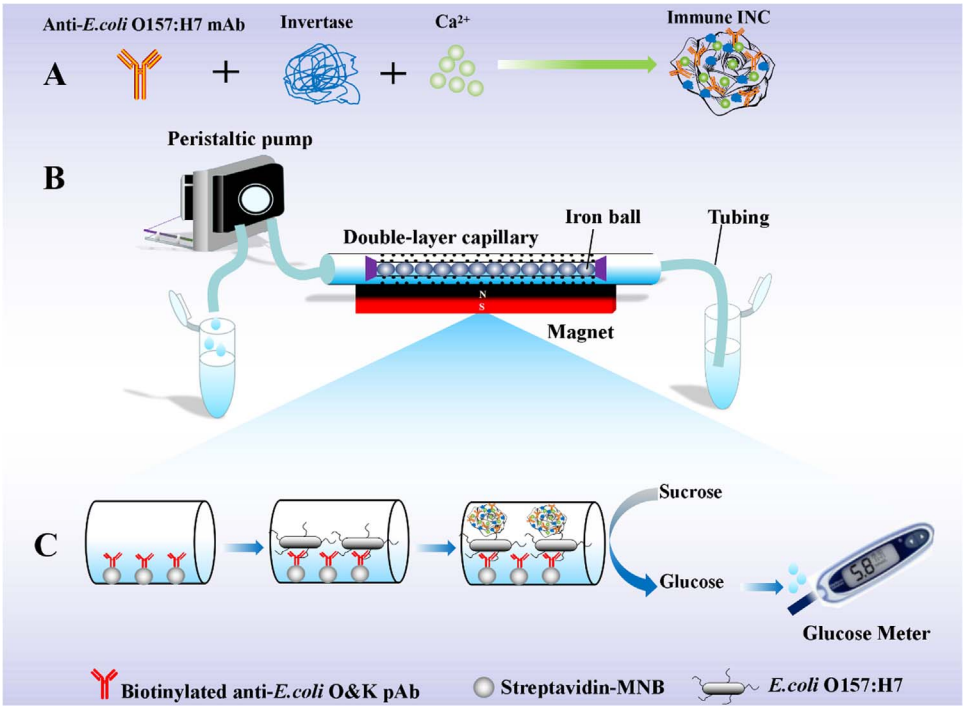

Fig. 1. Schematic of this proposed biosensor using double-layer capillary based immunomagnetic separation and invertase-nanocluster based signal amplification for rapid and sensitive detection of *E. coli* O157:H7.

2.4. Dot-ELISA test of the antibodies and the immune invertase-nanoclusters

Dot-ELISA test was conducted to evaluate the affinity of these two antibodies (the pAbs and the mAbs) against *E. coli* O157:H7. Based on the protocol reported in our previous study (Lin et al., 2015), 5 μL of the pAbs (0.4–0.5 mg/mL) and 5 μL of the mAbs (0.219 mg/mL) were used as the positive control, respectively, and 5 μL of PBS was used as the negative control. 5 μL of different concentrations of *E. coli* O157:H7 were used for the affinity test on the nitrocellulose membrane.

Besides, the conjugation of the mAbs onto the INCs was also verified using Dot-ELISA. 5 μL of the mAbs and 5 μL of PBS were used as the positive control and the negative control, respectively. Different amounts of the mAbs from 0.03 mg to 0.01 mg were used to prepare the immune INCs, respectively, and 5 μL of each immune INCs were used for the Dot-ELISA test on the nitrocellulose membrane.

2.5. Separation and concentration of the target bacteria

The separation and concentration of the target bacteria from the sample was conducted in the double-layer capillary, which consisted of an inner capillary (internal diameter: 1.0 mm; external diameter: 1.2 mm; length: 200 mm) with line-up iron balls (diameter: 0.8 mm) and an outer capillary (internal diameter: 1.8 mm; external diameter: 2.0 mm; length: 300 mm). Each end of the inner capillary was connected to a cylinder aligner with six holes, which was fabricated by a 3D printer (Objet 24, Stratasys, Eden Prairie, MN, USA) and used to be concentric with the outer capillary. Two repelling N35 neodymium magnets (length: 200 mm; width: 10 mm; thickness: 5 mm) were set up to generate a strong magnetic field and used to magnetize the iron balls. Many local HGMFs surrounding the iron balls were obtained and used to capture the immune MNBs in the capillary, when the immune MNBs were pumped into the capillary using a precise peristaltic pump (Type: T60-S2 & WX10-14-A, flowrate: 0–24 mL/min, Longer Pump, Baoding, Hebei, China).

Prior to separation of the target bacteria, the double-layer capillary was successively rinsed with alcohol (75%) one time and the deionized water three times, and then blocked with BSA (1%) for 30 min, followed by thoroughly washing with the deionized water. Besides, 50 μL of the streptavidin coated MNBs (Fe content: 1 mg/mL) were washed with PBS three times using the magnetic separator (MS0206, Aibit Biotech, Jiangyin, China), and re-suspended in 100 μL of PBS containing 20 μL of the biotinylated pAbs (0.4–0.5 mg/mL), followed by incubation at 15 rpm for 30 min. After magnetic separation to remove the surplus pAbs, the immune MNBs were re-suspended in 50 μL of PBS. The prepared immune MNBs were injected into the capillary with a flow rate of 1.2 mL/min at the presence of the magnetic field and recycled three times to ensure that most of the MNBs were captured and distributed uniformly in the capillary. Then, 1 mL of the *E. coli* O157:H7 sample at different concentrations (10^2–10^7 CFU/mL) was injected into the capillary and recycled for 45 min to ensure that most of the *E. coli* O157:H7 cells were captured by the immune MNBs through antigen-antibody binding. The capillary was finally washed with 5 mL of the deionized water at a flow rate of 0.36 mL/min to remove the residual sample background.

2.6. Detection of the target bacteria in pure cultures

The detection of the target bacteria was based on the forming of the MNB-bacteria-INC sandwich complexes using the immune INCs and the immune MNBs, the catalysis of the sucrose into the glucose by the invertase on the complexes, and the determination of the glucose using the glucose meter.

After the target bacteria were captured by the immune MNBs in the capillary, 50 μL of the prepared immune INCs, which was diluted 10 times prior to use, were injected into the capillary and recycled for 45 min. The immune INCs would react with the target bacteria to form the MNB-bacteria-INC complexes, followed by washing with 1 mL of the deionized water at the flow rate of 0.36 mL/min six times to remove the unbound immune INCs for better background noise control. Then, 100 μL of the sucrose (500 mM, pH 4.5) was injected into the capillary

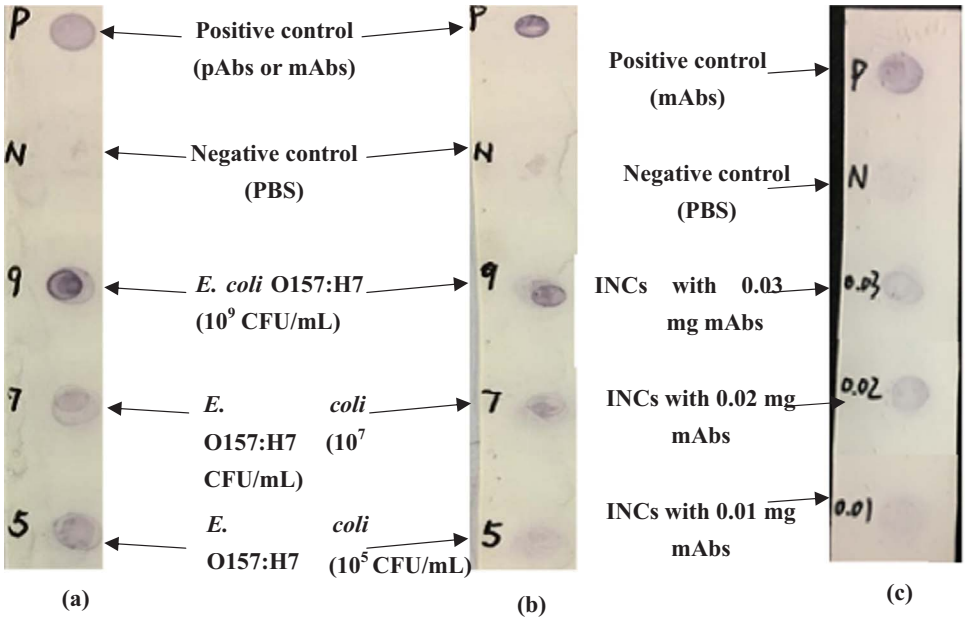

Fig. 2. Dot-ELISA analysis on the polyclonal antibodies (a), the monoclonal antibodies (b) and the immune invertase-nanoclusters (c).

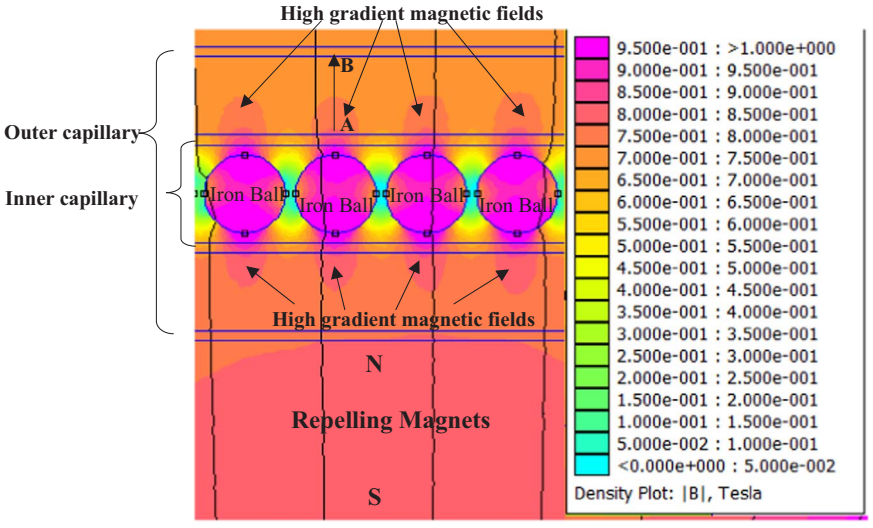

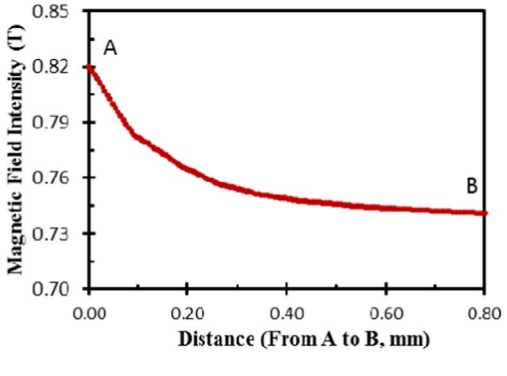

Fig. 3. (a) The simulation on the distribution of the magnetic field in the double-layer capillary; (b) the intensity of the high gradient magnetic field at different distances from the outer wall of the inner capillary.

and recycled for 30 min, allowing the invertase to catalyze the sucrose into the glucose. Finally, the glucose was collected and determined by the glucose meter to calculate the amount of the bacteria.

2.7. Detection of the target bacteria in the spiked milk

The pasteurized milk was purchased from a local supermarket and used as real sample model. Prior to use, the milk was diluted 10 times with the sterile PBS. 100 μL of the *E. coli* O157:H7 cells with the concentrations from 10^2 to 10^7 CFU/mL were mixed with 900 μL of the diluted milk to prepare the *E. coli* spiked milk samples. The *E. coli* O157:H7 cells in the spiked milk samples were first separated and concentrated using the double-layer capillary with the immune MNBs. Then, the immune INCs were used to react with the bacteria in the capillary and catalyze the sucrose into the glucose. Finally, the glucose was collected and detected using the glucose meter and the amount of the *E. coli* O157:H7 cells in the spiked milk was calculated using the calibration curve of this proposed biosensor.

3. Results and discussions

3.1. Dot-ELISA analysis of the antibodies and the immune invertase-nanoclusters

The affinity of the monoclonal antibodies and the polyclonal antibodies against *E. coli* O157:H7 is crucial to the sensitivity of this proposed biosensor. Therefore, Dot-ELISA test was conducted to evaluate the affinity of these two antibodies against the target bacteria. As shown in Fig. 2(a) and (b), there were visible dots for the positive control and the *E. coli* cells, and the dots became darker when the concentration of the *E. coli* cells increased, indicating that both the pAbs and the mAbs had good affinity to the *E. coli* O157:H7 cells.

Besides, the conjugation of the mAbs onto the INCs was also verified using Dot-ELISA. As shown in Fig. 2(c), dark dots were observed in the positive control and the INCs prepared with different amounts of the mAbs, indicating that the mAbs were successfully conjugated onto the INCs.

3.2. Simulation of the magnetic field in the double-layer capillary

The distribution of the high gradient magnetic fields in the double-layer capillary is very important to understand the locations for these magnetic fields to capture the MNBs. Finite Element Method Magnetics software was used to simulate the magnetic field. As shown in Fig. 3(a) and (b), when an enhanced magnetic field was generated by the two repelling cuboid magnets at their joint, the iron balls in the inner capillary could be magnetized to generate their individual HGMFs in the capillary. The mean intensity of each HGMF was around 0.76 T and the mean gradient of the HGMF was 100 T/m. To the best of our knowledge, many commercial magnetic separators generally had the maximum magnetic strength of ~ 0.35 T and the mean gradient of < 20 T/m for conventional immunomagnetic separation of biological targets, which were much weaker than these HGMFs for magnetic capturing of the immune MNBs. The separation efficiency of this proposed method was ~ 80% for *E. coli* O157:H7, which was comparable to the conventional magnetic separation method. The high separation efficiency might be attributed to the following reasons: (1) the higher capture efficiency of the MNBs in the capillary due to the presence of the HGMFs, resulting in a stronger magnetic force on the MNBs, (2) the more uniform distribution of the MNBs in the capillary due to the line-up iron balls, avoiding the aggregation of the MNBs and resulting in higher reaction efficiency between the antibodies on the MNBs and the target bacteria, and (3) the smaller space in the capillary for the target bacteria to flow through, resulting in faster diffusion of the bacteria into the whole channel and thus higher reaction efficiency between the antibodies on the MNBs and the target bacteria. Besides, the conventional magnetic separation methods can generally handle a small volume (1 mL or less) of bacterial samples with manual operations by well-trained technicians, however this proposed method has the potential to handle a larger volume up to 10 mL or more by an automatic or semi-automatic way.

3.3. Optimization of the catalytic reaction in the capillary

The pH and time of the catalytic reaction play important roles in the catalysis reaction and have great impact on the sensitivity of this proposed biosensor. Thus, the catalysis reaction of the sucrose into the glucose by the invertase was conducted at different pH conditions from 3.5 to 5.5 with the catalysis time of 30 min and the glucose was detected by the glucose meter right after the catalysis reaction was complete. As shown in Fig. 4(a), when the pH increased from 3.5 to 5.5, the readout of the glucose meter increased from 20.3 mM at the pH of 3.5, reached the peak of 32.2 mM at the pH of 4.5, and decreased to 27.6 mM at the pH of 5.5. Thus, the optimal pH of 4.5 was used in this study.

Besides, the catalysis reaction of the sucrose into the glucose by the invertase was conducted at different catalysis time from 7 min to 37 min with the optimal pH of 4.5, immediately followed by glucose detection using the glucose meter. As shown in Fig. 4(b), the readout of the glucose meter kept increasing from 5.4 mM to 27.8 mM while the catalysis time increased from 7 min to 30 min, and when the time was 37 min, the concentration of the catalyzed glucose was too high and the readout of the meter was out of the detection range (1.1–33.3 mM). Thus, the optimal catalysis time of 30 min was used in the study.

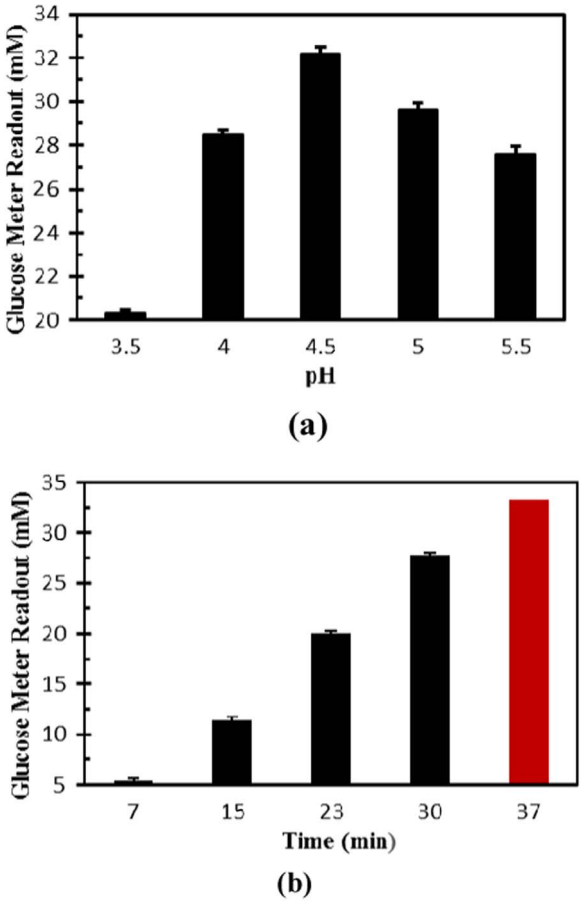

Fig. 4. Optimization of the pH (a) and time (b) for the enzymatic catalysis reaction.

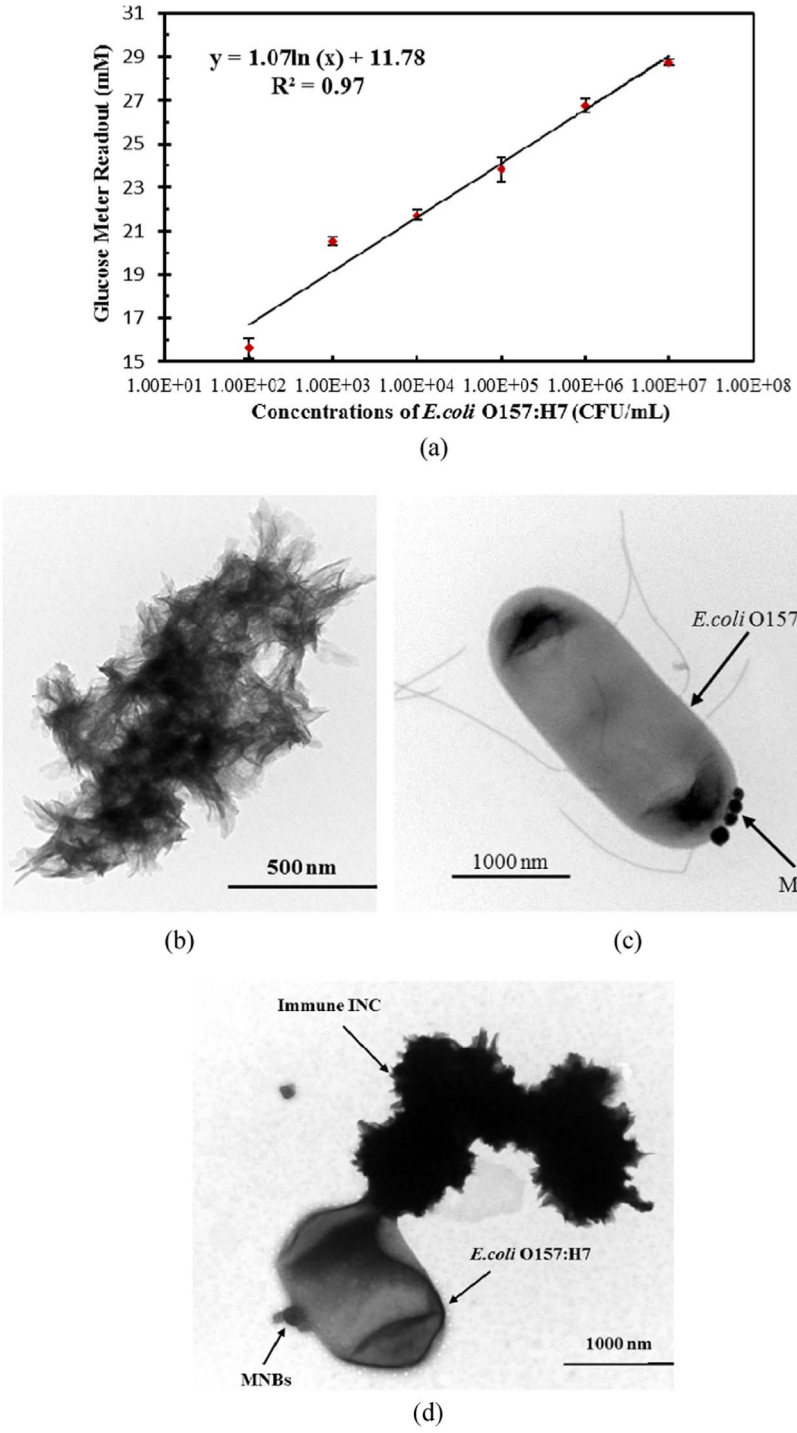

Fig. 5. Detection of the pure *E. coli* O157:H7 cultures using the proposed biosensor. (a) Calibration curve of the proposed biosensor; (b) TEM image of the immune INC; (c) TEM image of the MNB-*E. coli* complex; (d) TEM image of the MNB-*E. coli*-INC complex.

3.4. Modeling of this proposed biosensor for detection of E. coli O157:H7

The mathematic model of this proposed biosensor is the basis for the determination of the unknown concentration of *E. coli* O157:H7 in a sample. Thus, different concentrations of the *E. coli* O157:H7 cells from 1.0×10^2 CFU/mL to 1.0×10^7 CFU/mL were magnetically separated by the proposed double-layer capillary with the MNBs, catalyzed by the invertase on the sandwich complexes, and determined by the glucose meter. As shown in Fig. 5(a), a linear relationship between the readout of the glucose meter and the concentration of the *E. coli* O157:H7 cells from 1.0×10^2 CFU/mL to 1.0×10^7 CFU/mL was found and could be expressed as $y = 1.07 * \ln(x) + 11.78$ ($R^2 = 0.97$). The lower detection limit of this biosensor was determined to be 7.9×10^1 CFU/mL according to three times of signal-to-noise ratio, which was lower than that of the real-time quantitative PCR combined with magnetic silica beads based DNA extraction (~ 10^3 CFU/mL) and those of some recently reported biosensors combined with immune magnetic beads based bacteria separation (10^2–10^3 CFU/mL) for *E. coli* O157:H7 detection (Xu et al., 2016; Yang et al., 2015; Wu et al., 2017). The high sensitivity of this proposed biosensor could be attributed to two aspects: (1) the high separation efficiency of the target bacteria using the double-layer capillary with the immune MNBs, and (2) the high catalysis efficiency of the sucrose into the glucose due to the signal amplification using the immune invertase-nanoclusters.

To further confirm the forming of the MNB-bacteria-INC complexes, transmission electron microscope (TEM) was conducted. As shown in

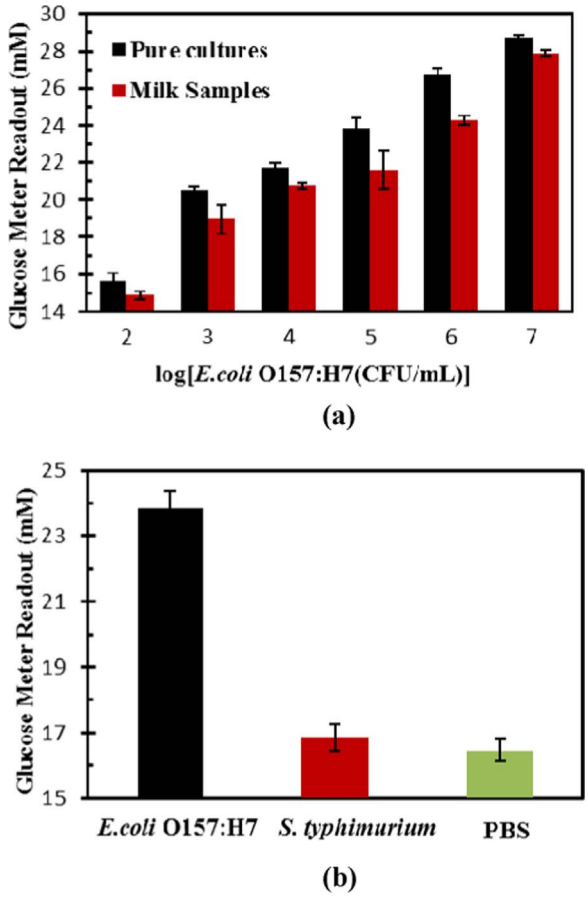

Fig. 6. (a) Detection of the spiked milk containing the *E. coli* O157:H7 cells with the concentrations from 1.0×10^2 to 1.0×10^7 CFU/mL; (b) detection of the *S. typhimurium* and *E. coli* O157:H7 at the same concentration of 1.0×10^5 CFU/mL, and the negative control.

Fig. 5(b)–(d), the INCs have an average size of 1–2 μm with flower-like nanostructures, the MNB-bacteria complexes and the MNB-bacteria-INC complexes were successfully formed.

3.5. Detection of E. coli O157:H7 in spiked milk

To further evaluate the applicability of this proposed biosensor, the pasteurized milk from the local supermarket was used as real sample model and 10-fold diluted by the sterile PBS. 100 μL of the *E. coli* O157:H7 cells at the concentrations from 1.0×10^2 to 1.0×10^7 CFU/mL were added into 900 μL of the prepared milk and then detected using this proposed biosensor. The pure *E. coli* O157:H7 cells at the same concentrations for the preparation of the spiked milk samples were also detected using this biosensor for calculating the recovery of the target bacteria. As shown in Fig. 6(a), the readouts of the glucose meter for the spiked milk samples containing the *E. coli* O157:H7 cells at different concentrations from 1.0×10^2 to 1.0×10^7 CFU/mL were slightly less than those for the original bacterial cells at the same concentrations. It was possibly due to the interference from the background of the milk samples since a large number of proteins, fats, and other molecules in milk might inhibit the separation of the target bacteria and the catalysis of the sucrose more or less (Wang et al., 2015). The recovery of the target bacteria (R) was calculated as the ratio of the concentration of the target bacteria in the spiked milk sample (Ns) to that of the bacteria in the pure culture (Nc), i.e. $R = Ns / Nc \times 100\%$. The recoveries for different concentrations of the target bacteria ranged from 80% to 94.8%, verifying the applicability of this proposed biosensor for detection of the *E. coli* O157:H7 in the milk.

Besides, *salmonella typhimurium* was used as non-target bacteria to evaluate the specificity of this proposed biosensor. The target bacteria (*E. coli* O157:H7) and the non-target bacteria at the same concentration of 1.0×10^5 CFU/mL, and the negative control (PBS) were detected using the proposed biosensor. As shown in Fig. 6(b), the readout of the glucose meter for the *S. typhimurium* cells was around 16.8 mM, which was close to that for the negative control (16.5 mM), while that for the *E. coli* cells was around 23.8 mM and much larger. This indicated that this proposed biosensor had a good specificity. The high readouts for *S. typhimurium* and negative control were due to the following reasons: (1) the immune invertase-nanoclusters with a large surface-to-volume ratio could greatly amplify the biological signal, resulting in a readable signal even from a very small amount of the invertase-nanoclusters residue; (2) excessive amount of the invertase-nanoclusters was used to reduce the analysis time in this study, resulting in more non-specific binding of the invertase-nanoclusters and thus leading to a high background noise level; (3) longer catalysis time was used to maximize the sensitivity of this biosensor in this study, resulting in more catalysate generated by the residual invertase-nanoclusters.

4. Conclusions

In this study, a novel biosensor combing double-layer capillary based high gradient immunomagnetic separation, invertase-nanocluster based signal amplification and glucose meter based signal detection, was successfully developed for sensitive and rapid detection of *E. coli* O157:H7. This proposed HGMS method had a separation efficiency of ~ 80% for *E. coli* O157:H7. This proposed biosensor had a wide linear detection range from 10^2 to 10^7 CFU/mL and was able to detect *E. coli* O157:H7 as low as 79 CFU/mL. Besides, this proposed biosensor might be extended for the detection of other foodborne pathogens and biological targets by changing the antibodies and it has the potential for rapid detection of foodborne pathogens in a larger volume of sample to further increase the sensitivity. However, this biosensor is still not ready for in-field application now due to some limitations, including (1) the fabrication of the coaxial capillary due to its frangibility; and (2) the background noise due to its non-specific adsorption, and needs to be further improved for practical applications.

Acknowledgments

This study was supported by the National Key Research and Development of China (2016YFD0201201) and Walmart Foundation (SA1703161).

References

Ahmed, A.M., Shimamoto, T., 2015. Int. J. Food Microb. 193 (10), 68–73.
Chen, H.W., Zhang, Z., Glennon, E., Ching, W.M., 2014. Bacteriology 3 (8), 1–6.
Chen, Q., Lin, J., Gan, C., Wang, Y., Wang, D., Xiong, Y., Lai, W., Li, Y., Wang, M., 2015. Biosens. Bioelectron. 74 (12), 504–511.
Chen, Q., Wang, D., Cai, G., Xiong, Y., Li, Y., Wang, M., Huo, H., 2016. Biosens. Bioelectron. 86 (7), 770–776.
Delaquis, P., Bach, S., Dinu, L.D., 2007. Food Prot. 70 (8), 1966–1974.
Dong, Z.M., Zhao, G.C., 2015. Talanta 137 (1), 55–61.
García, P.F., Brammen, M., Wolf, M., Reinlein, S., Roman, M.F.V., Berensmeier, S., 2015. Sep. Purif. Technol. 150 (8), 29–36.
Ge, J., Lei, J., Zare, R.N., 2012. Nat. Nanotechnol. 7 (7), 428–432.
Ghadeer, A.S., Sahar, A., Mohammed, Z., 2016. Biosens. Bioelectron. 92 (6), 702–708.
Gilbert, C., O'Leary, A., Winters, D., Slavik, M., 2015. Rapid Methods Autom. Microbiol. 11 (1), 61–74.
Huang, H., Liu, M., Wang, X., Zhang, W., Yang, D.P., Cui, L., Wang, X., 2016. Nanoscale Res. Lett. 11 (1), 507.
Khang, J., Kim, D., Chung, K.W., Lee, J.H., 2016. Talanta 147 (1), 177.
Li, Z., Fu, Y., Fang, W., Li, Y., 2015. Sensors Basel 15 (8), 19212–19224.
Lin, J., Li, M., Li, Y., Chen, Q., 2015. J. Magn. Magn. Mater. 378 (3), 206–213.
Nicola Luigi, B., Daniela, A., Donatella, P., Daniela, T., Ivana, V., Roberto, G., 2015. Adv. Protein Chem. Str. 101, 149–211.
Ozalp, V.C., Bayramoglu, G., Erdem, Z., Arica, M.Y., 2015. Anal. Chim. Acta 853 (1), 533–540.
Ren, W., Liu, W., Irudayaraj, J., 2017. Sens. Actuators B: Chem. 247 (8), 923–929.
Sharapov, U.M., Wendel, A.M., Davis, J.P., Keene, W.E., Farrar, J., 2016. Food Prot. 79 (12), 2024–2030.
Song, L., Zhang, L., Huang, Y., Chen, L., Zhang, G., Shen, Z., Zhang, J., Xiao, Z., Chen, T., 2017.

Sci. Rep. 7 (1), 3288.
Torso, L.M., Voorhees, R.E., Forest, S.A., Gordon, A.Z., Silvestri, S.A., Kissler, B., Schlackman, J., Sandt, C.H., Toma, P., Bachert, J., 2015. Food Prot. 78 (7), 1272–1279.
Vaisocherová-Lísalová, Hana, Víšová, Ivana, Ermini, Maria Laura, Špringer, Tomáš, Song, Xue Chadtová, Mrázek, Jan, Lamačová, Josefína, Lynn Jr., N.Scott, Šedivák, Petr, Homola, Jiří, 2016. Biosens. Bioelectron. 80 (3), 84–90.
Voetsch, A.C., Angulo, F.J., Rabatsky-her, T., 2004. Clin. Infect. Dis. Off. Publ. Infect. Dis. Soc. Am. 38 (3), S190–S197.
Wang, D., Chen, Q., Huo, H., Bai, S., Cai, G., Lai, W., Lin, J., 2016a. Food Control 73 (3), 555–561.
Wang, R., Lum, J., Callaway, Z., Callaway, Zach, Lin, J., Bottje, W., Li, Y., 2015. Biosens. Bioelectron. 5 (4), 791–803.
Wang, S., Xie, J., Min, J., Chang, K., Chen, R., Ma, L., Zhu, J., Guo, Q., Sun, H., Hu, J., 2016b. Sensors Basel 16 (11), 1856.
Wei, T.X., Du, Dan, Zhu, M.J., Lin, Y.H., Dai, Z.H., 2016. ACS Appl. Mater. Interfaces 8 (10), 6329–6335.
WHO, 2015. Food Safety. ⟨http://www.who.int/mediacentre/factsheets/fs399/en/⟩.
Wu, Y., Liu, Y., Zhan, Q., Liu, J., Li, R., 2017. AIP Adv. 7 (5), 056658.
Xu, M., Wang, R., Li, Y., 2016. Talanta 148 (8), 200–208.
Yang, Z., Sun, X., Wang, T., Lei, C., Liu, Y., Zhou, Y., Lei, J., 2015. Biomed. Microdevices 17 (1), 1–8.
Ye, R., Zhu, C., Song, Y., Lu, Q., Ge, X., Yang, X., Zhu, M.J., Du, D., Li, H., Lin, Y., 2016. Small 12 (23), 3094–3100.
Zhang, S., Zhu, X., Wu, Q., Zhang, J., Xu, X., Li, H., 2015. Ann. Microbiol. 65 (4), 1993–1999.
Zhang, X., Li, M., Zhang, B., Chen, K., He, K., 2016. PLoS One 11 (9), e0162274.
Zhang, Y., Tan, C., Fei, R., Liu, X., Zhou, Y., Chen, J., Chen, H., Zhou, R., Hu, Y., 2014. Anal. Chem. 86 (2), 1115–1122.
Zheng, X., Wang, Y., Lu, D., 2015. Miner. Eng. 79 (8), 94–101.
Zhu, L., Jing, H., Cao, X., Huang, K., Luo, Y., Xu, W., 2016. Sci. Rep. 6 (3), 16092.